

Angular distributions of selected N₂ Auger transitions

Q. Zheng, A. K. Edwards, R. M. Wood, and M. A. Mangan

Department of Physics and Astronomy, The University of Georgia, Athens, Georgia 30602

(Received 10 March 1995)

The angular distribution of Auger electrons produced in the collision of 1634-eV electrons with N₂ is reported. The angular distributions are measured relative to the internuclear axis of the molecule from 0° to 90° in 6° steps. When an Auger transition occurs to an unstable doubly ionized state the molecular ion dissociates into two N⁺ fragments. Because the time required for dissociation of the N₂²⁺ ion is much less than that for rotation of the ion, the axial recoil approximation holds to first order, and detecting one of the N⁺ ions determines the orientation of the target molecule at the time of the projectile-molecule collision. Therefore, a coincidence experiment between the Auger electrons of appropriate energy and the N⁺ fragments is devised. The rotation of the N₂²⁺ ions during the course of the dissociation process has been taken into account as a second-order approximation. As a result of this rotational effect, the predicted angular distribution function is smeared out by an amount depending on the different N₂²⁺ final states. The data are analyzed in terms of a two-center model in which prolate spheroidal coordinates are used.

PACS number(s): 33.80.Eh, 34.80.Gs

I. INTRODUCTION

It is well known that electrons emitted by atomic Auger transitions of *K*-shell vacancies have an isotropic angular distribution [1–4] because of the spherical symmetry of the atomic case. However, unlike the atomic case, the electrons emitted by molecular Auger transitions from *K*-shell vacancies of diatomic molecules are not expected to be isotropic [5]. First of all, the σ symmetry of the initial hole state does not have spherical symmetry nor do any of the final states; an Auger transition in a diatomic molecule is a two-center problem. Also, the angular distribution of the Auger electron in the laboratory frame depends on the orientation of the internuclear axis of the molecule at the time of the transition. If the formation of the initial hole state in the molecule depends on orientation, as it does in the photoexcitation process with polarized light, then the angular distributions of the ejected electrons are nonisotropic.

Early experiments on *K*-shell ionization by fast projectiles were done about 20 years ago and were directed toward making high-resolution measurements of Auger electron energies [6–8] and measurements of cross sections [9] for *K*-shell ionization. Measurements of the angular distribution of Auger electrons in these experiments were not made.

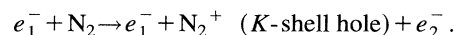
Since then much work, both experimental and theoretical, has been done on *K*-shell ionization and *K*-shell excitation of diatomic molecules. Most of the synchrotron-based studies that have been interested in angular distribution have focused on the $1s \rightarrow \pi^*$ discrete resonance and $1s \rightarrow \sigma_u$ shape resonance of N₂ and CO [10–16]. The discrete resonance is preferentially populated in molecules with the internuclear axis oriented perpendicular to the polarization vector while the shape resonance is preferentially populated for molecules oriented parallel to the polarization vector.

Other measurements that have used an electron-photoion coincidence technique [17,18] or a photoion-photoion coincidence [19,20] technique have dealt with identifying the states involved in the Auger transitions. We report here angular distribution measurements of molecular Auger elec-

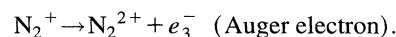
trons from selected transitions in N₂. The initial state vacancy is produced by a beam of fast electrons. A coincidence technique was developed to measure the angular distribution relative to the internuclear axis of the parent molecule.

II. EXPERIMENTAL PROCEDURE

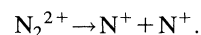
The time evolution of the process studied in this work is as follows. First, a nitrogen molecule in the ground vibrational level is bombarded by a fast electron and a *K*-shell vacancy is created, that is,



Second, the N₂⁺ ion undergoes an Auger transition in which one electron from an outer shell fills the *K*-shell hole and simultaneously a second electron is ejected:



Finally, the N₂²⁺ ion dissociates into two equal energy N⁺ ions



The objective of our experiment is to measure the angular distribution of Auger electrons emitted by the nitrogen molecules. In order for the angular distribution measurements to be meaningful the experiment must be able to detect the Auger electrons from those molecules with a particular orientation in space. Because the time required for dissociation of the unstable N₂²⁺ ion into two N⁺ ions is shorter than that for rotation of the ion, the axial recoil approximation holds to first order. This implies that the two N⁺ ions formed in the dissociation travel outward approximately along the internuclear axis of the N₂ molecule. Therefore, detecting one of the

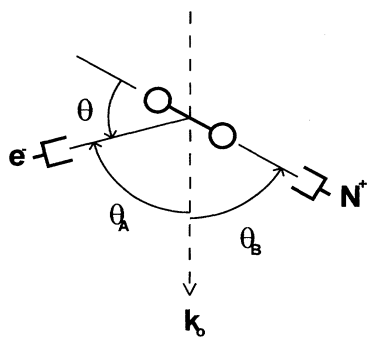


FIG. 1. Schematic diagram of the scattering geometry. Auger electrons and N⁺ fragments from the target gas N₂ are energy analyzed and their relative times of flight from the collision region to the detector are measured.

N⁺ fragments is a measure of the orientation of the molecule at the time of the projectile-molecule collision, the Auger decay, and the molecular dissociation.

In order to take advantage of the fact that the molecular orientation is indicated by the trajectory of the N⁺ ion, a coincidence experiment between the Auger electrons and N⁺ fragments is devised to measure the angular distribution of the Auger electrons relative to the direction of the internuclear axis of their parent molecules.

The schematic diagram of the collision region is shown in Fig. 1. The N⁺ detector is set at angle θ_B and the Auger electron detector at θ_A with respect to the incident electron-beam direction. Both detectors are free to rotate independently in the plane defined by the projectile beam and detectors. During the measurements of the angular distributions, the angle θ_B is fixed and the angle θ_A is varied so that the angle θ , defined as the angle between the direction taken by the Auger electron and the internuclear axis, is varied from 0° to 90° in 6° steps.

The energy of the bombarding electrons is 1634 eV. The beam of electrons enters a differentially pumped collision region and is collected in a Faraday cup and integrated. The N₂ pressure in the collision region during the collection of data is approximately 10⁻⁴ Torr, which means that the effect of multiple collisions is negligible.

In our experiment, the N⁺ ions and the Auger electrons are energy analyzed by identical hemispherical, electrostatic analyzers and detected by channel electron multipliers. The transmission function of the analyzers is triangular in shape with a full width at half maximum (FWHM) of 1.5% of the energy at which the ion or electron is analyzed. In this work, the N⁺ ions were accelerated by a set of focusing elements and analyzed at ten times their initial energy and the Auger electrons were slowed down by a similar set of focusing elements and analyzed at half their initial energy.

Standard time-of-flight techniques are used to record electron-ion coincidences. Whenever an electron is detected by the channel electron multiplier, a time-to-amplitude converter (TAC) is started. The stop pulse for the TAC is derived from the N⁺ detector. The height of the output pulse from the TAC is proportional to the length of time elapsed be-

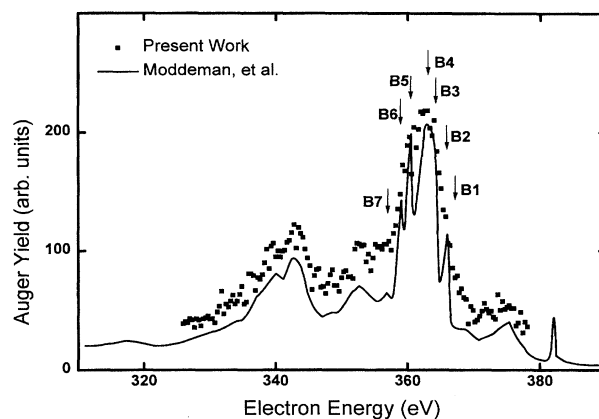


FIG. 2. Molecular nitrogen K-shell Auger electron spectrum produced by bombardment of N₂ by a beam of 1634-eV electrons. The highest peak is the B4 peak at 362.5 eV. The solid curve is the experimental Auger spectrum of Moddeman *et al.* [8].

tween the start and stop inputs. This signal is processed by an analog-to-digital converter and recorded in a multichannel analyzer.

The molecular nitrogen Auger electron spectrum in the 357–370 eV region obtained in this work is shown in Fig. 2. The overall features of our Auger electron spectrum are in agreement with the result of Moddeman *et al.* [8], except for the fact that their energy resolution was 0.09% FWHM and their spectrum shows more detailed structure than ours. The energy axis of the Auger electron spectrum was calibrated using known peaks in Moddeman's Auger spectrum.

Figure 3 shows the kinetic-energy distribution of N⁺ ions obtained in this work. No efficiency correction has been made to the data. The N⁺ energy spectrum is a superposition of several overlapping channels due to the ionization of N₂ molecules and their subsequent dissociation. The spectra shown in Figs. 2 and 3 are recorded without imposing any coincidence requirement.

In the experiment, we concentrate on the most intense

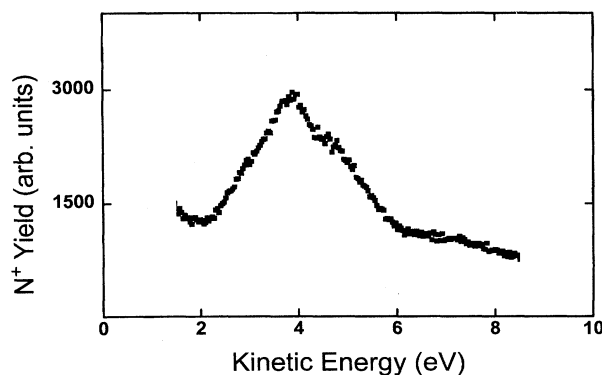


FIG. 3. N⁺ kinetic-energy spectrum from the dissociation of ionized N₂. The energy released from the dissociation of N₂²⁺ is shared by two N⁺ ions according to the conservation of momentum.

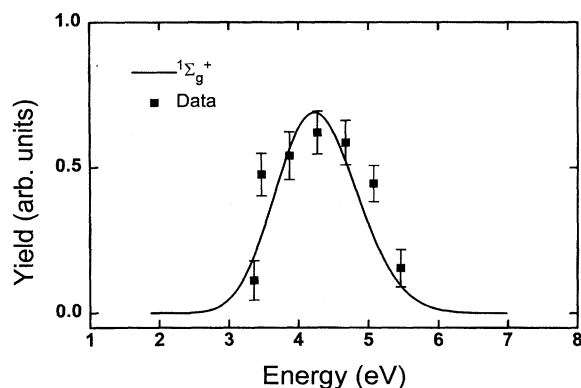


FIG. 4. N^+ ion and 362.5-eV Auger electron coincidence yield as a function of N^+ -ion energy. The solid curve represents the reflection approximation prediction of the shape of the energy spectrum produced by ionization and subsequent dissociation through the channel $N_2^{2+}(1\pi_u^{-2})^1\Sigma_g^+ \rightarrow N^+(^3P) + N^+(^3P)$. Thermal and instrumental broadening has been included.

Auger transition in the N_2 Auger spectrum for which the kinetic energy of the Auger electron is 362.5 eV. This transition is known as the B4 peak in the literature [8]. The voltage settings on the electron detector were fixed to analyze the Auger electrons centered on B4 and the energy resolution at these settings was 2.7 eV (FWHM). According to Moddeman's Auger spectrum, the energy separations between the center of the B4 peak and those of the nearby peaks B3 and B5 are 1 and 2.3 eV, respectively. Consequently, the B4 peak in this work may be contaminated with some B3, if the final state is dissociative, and B5 yield. The relatively poor energy resolution in our work enables us to conduct the experiment in a reasonable amount of time.

The voltage settings on the N^+ analyzer were varied in order to maximize the coincidence yield. Figure 4 shows the Auger electron- N^+ -ion coincidence yield as a function of the energy setting on the N^+ analyzer. The error flags indicate statistical uncertainties only. The presence of the peak near 4.3 eV in the coincidence spectrum infers the existence of the dissociation channel $N_2^{2+} \rightarrow N^+ + N^+ + 8.6$ eV. The 8.6-eV energy release is consistent with the predicted values from the dissociation of the $N_2^{2+}(1\pi_u^{-2})^1\Delta_g$ and $^1\Sigma_g^+$ and $(2\sigma_u^{-1}1\pi_u^{-1})^3\Pi_g$ states. The solid curve in the figure represents the reflection approximation prediction of the profile of the energy spectrum calculated from the dissociation of the $N_2^{2+}(1\pi_u^{-2})^1\Sigma_g^+$ state by using O'Neil's N_2^{2+} potential-energy curve [21]. More detailed discussions of the reflection approximation are given elsewhere [22,23]. The measured coincidence spectrum is in good agreement with the theoretical reflection approximation prediction.

The N^+ -energy analyzer is set at the peak of the coincidence yield shown in Fig. 4. The amount of charge collected during one run of the coincidence experiments is recorded as well as the total number of N^+ fragments and the total number of Auger electrons detected in that run. The ratios of the N^+ counts and electron counts to the total charge are monitored to ensure the reliability of the data. The number of the true coincidences between N^+ fragments and Auger electrons is normalized to the total number of N^+ fragments in

order to eliminate the effects of some fluctuation in the pressure, temperature, and projectile beam current during the experiment.

As the electron analyzer is moved in angle while the N^+ analyzer is held fixed, the common beam length observed by both analyzers changes. It is a minimum at $\theta_A = 90^\circ$ ($\theta = 30^\circ$) and a maximum at $\theta_A = 30^\circ$ ($\theta = 90^\circ$). In front of the focusing elements of the analyzers are two slits that define the effective beam length observed and the angular acceptance of each analyzer. Any rays emanating from the collision region that pass through the slits at a selected energy are focused into the energy analyzers. Only those points along the beam that can contribute counts to both analyzers are included in finding a common acceptance of the two systems [24]. The total number of coincidences at each angle are corrected by normalizing to the common acceptance at $\theta_A = 90^\circ$ ($\theta = 30^\circ$).

III. THEORY

The process of inner-shell ionization followed by emission of an Auger electron is usually interpreted as a two-step process in which the decay is treated independently of the primary ionization. Because the $1\sigma_g$ and $1\sigma_u$ levels of nitrogen have practically the same binding energy, it is assumed that $1\sigma_g$ and $1\sigma_u$ holes are equally likely to be formed in the primary projectile-electron collision.

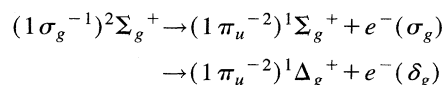
The transition moment for the Auger decay is

$$T_{fi} = \langle \Psi_f | r_{12}^{-1} | \Psi_i \rangle,$$

where r_{12}^{-1} is the Coulomb interaction between the two electrons that participate directly in the Auger transition and Ψ_f and Ψ_i are two-electron wave functions for the final and initial states, respectively. The angular distribution of the Auger electron in the molecular frame can be found by solving for T_{fi} in the frame of the molecule, taking its square, and integrating over the azimuthal angle ϕ of the exiting Auger electron.

Our experiment concentrates on the strongest transition in the Auger spectrum at 362.5 eV [8]. In order for this Auger transition to be detected in the coincidence experiment, it is necessary that the final state be a dissociative state. The calculations of Wetmore and Boyd [25] and O'Neil [21] show that the $(1\pi_u^{-2})^1\Delta_g$, $^1\Sigma_g^+$, and $(2\sigma_u^{-1}1\pi_u^{-1})^3\Pi_g$ states of N_2^{2+} are in the proper range of energies for the B4 peak and are dissociative in the Franck-Condon region.

The symmetry of the wave function of the Auger electron is found by taking the direct product of irreducible representations of the electron and the final states. For example, assume that the initial hole is $1\sigma_g^{-1}$. Then, for the transitions of interest,



or

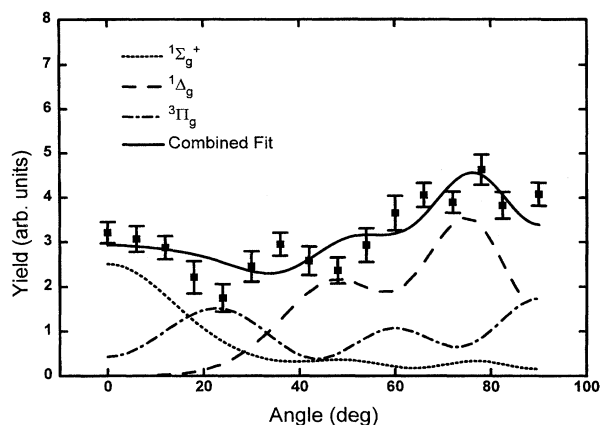


FIG. 5. Angular distribution of 362.5-eV Auger electrons in coincidence with N⁺ ions from the dissociation of N₂²⁺ as a function of θ defined in the text. The fits are explained in the text.

$$(1\sigma_g^{-1})^2\Sigma_g^+ \rightarrow (2\sigma_u^{-1}1\pi_u^{-1})^3\Pi_g + e^-(\pi_g).$$

The direct product of the irreducible representations for the Auger electron and the N₂²⁺ state must contain the irreducible representation of the initial hole state. If the initial hole is $1\sigma_u^{-1}$ then the inversion symmetry of the Auger electron changes from g to u .

Only general features of the angular distribution of Auger electrons can be determined from the symmetry of their wave functions. Namely, if the outgoing wave has σ symmetry, then electrons will appear along the internuclear axis, and if the inversion symmetry is ungerade, then the wave has a node at 90° relative to the axis and no electrons will be emitted in that direction. If the symmetry is gerade, then it has an antinode at 90° and electrons are found. In order to learn specific details of the angular distribution it is necessary to evaluate the transition moment and determine the contributions for each partial wave of a given azimuthal quantum number m .

The symmetry arguments given above apply in the evaluation of T_{fi} . For example, when a $1\pi_u$ electron falls into a $1\sigma_g$ hole, then the r_{12}^{-1} interaction must have π_u symmetry or else the transition moment vanishes. With an interaction of π_u symmetry and, if the Auger electron is ejected from the $1\pi_u$ orbital, then it can be either σ_g or δ_g . Similar arguments apply for a $1\sigma_u$ hole.

An evaluation of T_{fi} is presented in the following paper [26]. An angular distribution is calculated in prolate spheroidal coordinates for each transition and fit to the experimental results.

IV. RESULTS AND DISCUSSION

Figure 5 presents the angular distribution of the Auger electrons emitted by the nitrogen ions that were produced by bombardment of the nitrogen molecules with the 1634-eV electrons. The yield is plotted as a function of the angle θ as

defined in Fig. 1. The error flags indicate statistical uncertainties only. The data were obtained with the N⁺ analyzer set at 60° relative to the incident beam. We also measured the Auger electron angular distributions with the angle of θ_B set at 90° and 120°. Although these data were less complete because of spatial restriction on the moving of the detectors within the chamber, they were consistent with the data shown in Fig. 5 within the errors flags. While the angle θ_B was set at 90°, the angular distribution was measured as the electron detector moved from one side of the molecular internuclear axis to the other side in 6° steps. It is found that the results were symmetric within the statistical errors about the line defined by $\theta=0^\circ$. This is consistent with our expectation that the emission of the Auger electrons from the nitrogen molecules is independent of the azimuthal angle.

Before the angular distribution function outlined in Sec. III is fit to the data, the corrections caused by the rotational motion of N₂²⁺ ions need to be made. It is found that the angular distribution function is smeared out by an amount depending on the different N₂²⁺ final states, the N₂²⁺ dissociation lifetime, the moments of inertia of the molecule, and the rotational temperature. A more detailed discussion of the rotational effect will be presented elsewhere. The modified distribution functions of the different N₂²⁺ final states are used in a least-squares fitting routine to analyze the data. The results are shown in Fig. 5. The fitting procedure varies the relative amount of the transitions to the N₂²⁺($1\pi_u^{-2}$)¹ Δ_g , ¹ Σ_g^+ , and ($2\sigma_u^{-1}1\pi_u^{-1}$)³ Π_g final states to minimize the χ^2 in the fit routine.

The dotted curve in Fig. 5 represents the contribution of the transition to the N₂²⁺($1\pi_u^{-2}$)¹ Σ_g^+ final state, the dashed curve represents the transition to the N₂²⁺($1\pi_u^{-2}$)¹ Δ_g final state, and the dash-dotted curve represents the transition to the N₂²⁺($2\sigma_u^{-1}1\pi_u^{-1}$)³ Π_g final state. The solid curve is the fitted profile to the data from the three different N₂²⁺ states. The combined fit represents the general features of the experimental data. The individual contributions to the full fit from the transitions to the N₂²⁺($1\pi_u^{-2}$)¹ Σ_g^+ state is 12%, 60% to the N₂²⁺($1\pi_u^{-2}$)¹ Δ_g state, and 28% to the N₂²⁺($2\sigma_u^{-1}1\pi_u^{-1}$)³ Π_g state. These numbers are obtained by integrating each corresponding curve over $\sin\theta d\theta$ from 0° to 90° and normalizing to the solid curve.

It is interesting to note that the predicted angular distribution function of the transition to the ¹ Σ_g^+ state is the only one of the transitions to the three final states considered having yield at 0° before rotational corrections are made. This is easily seen by expanding the prolate spheroidal function for the σ Auger electron in associated Legendre functions. Only $m=0$ Legendre functions contribute to the expansion. After the rotational corrections are made, a contribution at 0° occurs for the transition to the ³ Π_g final state as shown in Fig. 5.

ACKNOWLEDGMENTS

The authors would like to thank Dr. M. M. Duncan and Dr. H. Nakamura for helpful discussions. This work is supported by the National Foundation under Grant No. PHY-9307129.

- [1] W. Mehlhorn, Phys. Lett. **26A**, 166 (1968).
- [2] B. Cleff and W. Mehlhorn, Phys. Lett. **37A**, 3 (1971).
- [3] S. Flügge, W. Mehlhorn, and V. Schmidt, Phys. Rev. Lett. **29**, 7 (1972).
- [4] B. Cleff and W. Mehlhorn, J. Phys. B **7**, 593 (1974).
- [5] D. Dill, J. R. Swanson, S. Wallace, and J. L. Dehmer, Phys. Rev. Lett. **45**, 1393 (1980).
- [6] K. Siegbahn, C. Nordling, G. Johansson, J. Hedman, P. F. Hedén, K. Hamrin, U. Gelius, T. Bergmark, L. O. Werme, R. Manne, and Y. Bear, *ESCA, Applied to Free Molecules* (North-Holland, Amsterdam, 1971).
- [7] D. Stalherm, B. Cleff, H. Hilling, and W. Mehlhorn, Z. Naturforsch. Teil A **24**, 1728 (1969).
- [8] W. E. Moddeman, T. A. Carlson, M. O. Krause, B. P. Pullen, W. E. Bull, and G. K. Schweitzer, J. Chem. Phys. **55**, 2317 (1971).
- [9] N. Stolterfoht, D. Schneider, and K. G. Harrison, Phys. Rev. A **8**, 2363 (1973).
- [10] D. W. Lindle, C. M. Truesdale, P. H. Korbin, T. A. Ferrett, P. A. Heimann, U. Becker, H. G. Kerkhoff, and D. A. Shirley, J. Chem. Phys. **81**, 5375 (1984).
- [11] U. Becker, R. Hölzel, H. G. Kerkhoff, B. Langer, D. Szostak, and R. Wehlitz, Phys. Rev. Lett. **56**, 1455 (1986).
- [12] N. Saito and I. H. Suzuki, Phys. Rev. Lett. **61**, 2740 (1988); J. Phys. B **22**, 3973 (1989).
- [13] A. Yagishita, H. Maezawa, M. Ukai, and E. Shigemasa, Phys. Rev. Lett. **62**, 36 (1989).
- [14] E. Shigemasa, K. Ueda, Y. Sato, T. Sasaki, and A. Yagishita, Phys. Rev. A **45**, 2915 (1992).
- [15] D. L. Lynch, Phys. Rev. A **43**, 5176 (1991).
- [16] O. Hemmers, F. Heiser, J. Eiben, R. Wehlitz, and U. Becker, Phys. Rev. Lett. **71**, 987 (1993).
- [17] W. Eberhardt, E. W. Plummer, I.-W. Lyo, R. Carr, and W. K. Ford, Phys. Rev. Lett. **58**, 207 (1987).
- [18] D. M. Hanson, C. I. Ma, K. Lee, D. Lapiano-Smith, and D. Y. Kim, J. Chem. Phys. **93**, 9200 (1990); Chem. Phys. **162**, 439 (1992).
- [19] N. Saito and I. H. Suzuki, J. Phys. B **20**, L785 (1987).
- [20] M. J. Besnard, L. Hellner, G. Dujardin, and D. Winkoun, J. Chem. Phys. **88**, 1732 (1988).
- [21] S. V. O'Neil (private communication).
- [22] G. H. Dunn and L. J. Kieffer, Phys. Rev. **132**, 2109 (1963).
- [23] A. S. Coolidge, H. M. James, and R. D. Present, J. Chem. Phys. **4**, 193 (1936).
- [24] Q. Zheng, Ph.D. dissertation, The University of Georgia, 1995 (unpublished).
- [25] R. W. Wetmore and R. K. Boyd, J. Phys. Chem. **90**, 5540 (1986).
- [26] Q. Zheng, A. K. Edwards, R. M. Wood, M. A. Mangan, following paper, Phys. Rev. A **52**, 3945 (1995).